

Usefulness of Integrated PET/MRI in Head and Neck Cancer: A Preliminary Study

Soo Jin Lee · Hyo Jung Seo · Gi Jeong Cheon ·
Ji Hoon Kim · E. Edmund Kim · Keon Wook Kang ·
Jin Chul Paeng · June-Key Chung · Dong Soo Lee

Received: 5 July 2013 / Revised: 4 November 2013 / Accepted: 7 November 2013 / Published online: 6 December 2013
© Korean Society of Nuclear Medicine 2013

Abstract

Purpose The new modality of an integrated positron emission tomography/magnetic resonance imaging (PET/MRI) has recently been introduced but not validated. Our objective was to evaluate clinical performance of ^{18}F -fluoro-2-deoxyglucose (^{18}F -FDG) PET/MRI in patients with head and neck cancer. **Methods** This retrospective study was conducted between January 2013 and February 2013. Ten patients (eight men, two women; mean age, 61.4 ± 13.4 years) with histologically proven head and neck tumors were enrolled. Whole-body PET/MRI and regional positron emission tomography (PET) with dedicated MRI were sequentially obtained. Maximum standardized uptake value (SUVmax), SUVmean, metabolic tumor volume, total

lesion glycolysis and contrast enhancement were analyzed. A total of ten whole-body positron emission tomography (PET), ten regional positron emission tomography (PET), ten dedicated MRI and ten regional PET/gadolinium-enhanced T1-weighted (Gd)-MRI images were analyzed for initial staging. Two nuclear medicine physicians analyzed positron emission tomography (PET) and PET/MRI with a consensus. One radiologist analyzed dedicated MRI. The primary lesions and number of metastatic lymph nodes analyzed from each image were compared.

Results Eight patients were diagnosed with head and neck cancer (one tongue cancer, four tonsillar cancers, one nasopharyngeal cancer and two hypopharyngeal cancers) by histological diagnosis. Two benign tumors (pleomorphic adenoma and Warthin tumor) were diagnosed with surgical operation. Whole-body positron emission tomography (PET) and regional positron emission tomography (PET) attenuated by MRI showed good image quality for the lesion detection. Whole-body positron emission tomography (PET) and regional positron emission tomography (PET) detected ten primary sites and compensated for a missed lesion on dedicated MRI. A discordant number of suspicious lymph node metastases was noted according to the different images; 22, 16, 39 and 40 in the whole-body positron emission tomography (PET) only, dedicated MR, regional positron emission tomography (PET) only and regional PET/Gd-MRI, respectively. There was no distant metastasis based on analysis of whole-body positron emission tomography (PET) and whole-body PET/Dixon-volume interpolated breathhold examination (VIBE) MRI. Regional PET/Gd-MRI combined with whole-body PET/MRI modified staging in three patients. Lesions of primary tumor and suspicious metastasis were well detected on both value of SUVmax and visual analysis. The regional PET/Gd-MRI combined with whole-body PET/MRI showed convenient clinical staging performance compared with positron emission tomography (PET) and MRI alone.

Conclusion In this preliminary study, PET attenuated by MRI showed good image quality to detect lesions. And whole-body

S. J. Lee · H. J. Seo (✉) · G. J. Cheon (✉) · K. W. Kang ·
J. C. Paeng · J.-K. Chung · D. S. Lee
Department of Nuclear Medicine, Seoul National University
Hospital, 28 Yeongun-dong, Jongro-gu, Seoul 110-744, Korea
e-mail: sihun12@snu.ac.kr
e-mail: larrycheon@gmail.com

H. J. Seo · E. E. Kim · D. S. Lee
Department of Molecular Medicine and Biopharmaceutical Sciences,
WCU Graduate School of Convergence Science and Technology,
Seoul National University College of Medicine, Seoul, Korea

G. J. Cheon · K. W. Kang · J.-K. Chung · D. S. Lee
Cancer Research Institute, Seoul National University College of
Medicine, Seoul, Korea

J. H. Kim
Department of Radiology, Seoul National University Hospital, Seoul,
Korea

E. E. Kim
Department of Radiological Science, University of California at
Irvine, Irvine, CA, USA

G. J. Cheon
Department of Nuclear Medicine, Seoul National University College
of Medicine, 28 Yeongun-dong, Jongro-gu, Seoul 110-744, Korea

PET/MRI as a single modality was feasible for staging in a clinical setting. Whole-body positron emission tomography (PET), regional positron emission tomography (PET), dedicated MRI and regional PET/Gd-MRI showed discordant results in lesion detection. These discordant results might be synergistic effect for accurate staging.

Keywords Head and neck cancer · Oncology · PET · MRI · Integrated PET/MRI

Introduction

Positron emission tomography (PET) using ^{18}F -fluoro-2-deoxyglucose (FDG) has been known to be a useful tool to detect the malignancy in various cancers. PET has advantages for whole-body evaluation, which makes it possible to discover distant metastases. In the initial period, PET had a limitation to evaluate the loco-regional lesion due to difficulty of anatomical correlation. Also, these caused the problem to read PET image between the physiologic metabolism and malignant metabolism. Simply, these problems were widely resolved by the emergence of PET/CT. Combined computed tomography (CT) clarified whether the FDG uptake was metabolically active or not. CT showed better morphologic information and smaller lesion than PET. It improved the sensitivity and specificity of PET in staging and detection of recurrence [1, 2].

The head and neck have complex anatomy and involve many normal structures such as lymphoid tissue, laryngeal muscle and salivary glands. They induce variable patterns and intensity of FDG uptake. Malignancy in these organs is usually evaluated from endoscopy, contrast-enhanced CT and contrast-enhanced magnetic resonance imaging (MRI) [3]. PET/CT was useful to evaluate suspicious metastatic lymph nodes or recurrence in treated scarred areas which were detected from other images. Also, PET has similar accuracy to detect metastatic lymph nodes compared with dedicated CT and MRI [4] and is superior to other modalities for finding the primary malignant lesion in case of proven metastatic cervical lymph nodes. After integration of PET and CT, the characteristics of disease have been better demonstrated with combined anatomy and metabolism [5].

Progressive new imaging tool, PET/MRI potentially has the advantage of diagnosis in oncology. MRI shows increased soft tissue contrast compared with CT and has no radiation dose [6]. Integration of PET/MRI has been expected to improve sensitivity and specificity compared with PET/CT. Most of all, the sensitivity and accuracy for metastatic regional lymph nodes has been clinically concerned. Also detailed analysis using metabolic activity is possible in lesion-based analysis. Recently, many studies related to PET/MRI have been introduced [7–9]. These researches are in its early stage, and therefore the usefulness of integrated PET/MRI has not been fully evaluated.

Thus, in the current investigation, we retrospectively reviewed the PET/MRI of ten patients, diagnosed with head and neck tumor. We will describe the initial experience to compare the diagnosis and sensitivity of MRI attenuation-corrected PET images with that of integrated PET/MRI in head and neck cancer patients.

Materials and Methods

Patients

This study was approved by the Institutional Review Board (IRB) of Seoul National University Hospital (SNUH). Between January 2013 and February 2013, ten patients were retrospectively selected. They had been diagnosed with head and neck tumor at SNUH or an outside hospital. Patients were referred and underwent PET/MRI for staging of known tumors or for detecting unknown primary lesion. Patients' characteristics are listed in Table 1. Two benign tumors (pleomorphic adenoma and Warthin tumor) and one tonsillar cancer were confirmed by surgical operation. No patient had been treated for head and neck cancer previously. The PET/MRI and dedicated MRI images were obtained simultaneously. Based on the initial staging, clinicians decided to choose therapeutic modality.

Imaging Protocol

All acquisitions were performed by using an integrated PET/MRI scanner (Siemens Healthcare, Erlangen, Germany). All patients fasted for 6 h before the scan; serum glucose levels were obtained before the injection and were less than 200 mg/dl in all patients. 0.14 mCi/kg of ^{18}F -FDG was injected. Whole-body and regional PET images were sequentially obtained after once injection. At 50 min post injection, the patient was placed on the PET/MRI scanner bed. The MR examinations were performed with a 3-T MR imaging unit. Firstly, a simple fast sequence of MRI was performed for a scout image. Afterwards a whole-body PET scan was performed to cover from head to the distal thigh (craniocaudal). Each bed PET was performed with an acquisition time of 3 min, 25.7-cm bed length with 30 % of overlapping area, $4.1 \times 2.6 \times 3.1$ mm and 172 matrixes. Simultaneously, MR image acquisition was performed per bed. At first, MRI sequence to correct PET attenuation was performed. It was followed by Dixon-VIBE (volume interpolated breathhold examination) sequences in axial orientation and HASTE (half-Fourier acquisition single shot turbo spin echo) T2-weighted in coronal orientation. Whole-body MRI scan lasts 5 min 35 s per bed.

After whole-body PET/Dixon-VIBE MRI scan, regional PET and MRI images were performed. Regional PET was performed with an acquisition time of 10 min, a voxel size

Table 1 TNM Staging according to contrast-enhanced CT only, whole-body PET only, Gd-enhanced T1-weighted MRI, regional PET only, regional PET/Gd-MRI and whole-body PET/Dixon VIBE MRI + regional PET/Gd-MRI

| Patient | Primary tumor | Pathology | TNM stage | | | | | |
|---------|---------------|---------------------------|-----------|-----------|----------------|---------|-----------------|--|
| | | | CE-CT TN | WB PET NM | Gd-MRI TN | R-PET N | R-PET/Gd-MRI TN | WB PET/Dixon VIBE MRI + R-PET/Gd-MRI TNM |
| 1 | Parotid | Pleomorphic adenoma | - | - | - | - | - | - |
| 2 | Parotid | Warthin tumor | - | - | - | - | - | - |
| 3 | Tongue | SCC | - | N2bM0 | T4aN2b | N2b | T4aN2b | T4aN2bM0 |
| 4 | Tonsil | SCC, MD | - | N1M0 | TxN2b | N2b | T1N2b | T1N2bM0 |
| 5 | Tonsil | SCC | TxN2c | N2cM0 | T2N2c | N2c | T2N2c | T2N2cM0 |
| 6 | Tonsil | SCC, WD | T3/T4N0 | N2cM0 | T4bN2b | N2c | T4aN2c | T4aN2cM0 |
| 7 | Tonsil | SCC, MD | T2N2a | N2bM0 | T2N2b | N2b | T2N2b | T2N2bM0 |
| 8 | Nasopharynx | Non-keratinizing type, PD | TxN1 | N1M0 | T1N1 | N1 | T1N1 | T1N1M0 |
| 9 | Hypopharynx | SCC | T2N1 | N2bM0 | T3N2b | N2b | T3N2b | T3N2bM0 |
| 10 | Hypopharynx | SCC, MD | T4bN0 | N2bM0 | T2N0M1 or T3N0 | N2b | T4bN2b | T4bN2bM0 |

CE-CT contrast enhanced CT, WB PET whole-body PET, Gd-MRI Gd-enhanced T1-weighted MRI, R-PET regional PET, R-PET/Gd-MRI the integration of regional PET with Gd-enhanced T1-weighted MRI; SCC squamous cell carcinoma, WD well differentiated, MD moderately differentiated, PD poorly differentiated

of $1.6 \times 1.6 \times 1.6$ mm and 344 matrixes. Several MR sequences were simultaneously performed in head and neck. A transverse T2-weighted turbo spin echo (TSE) short T1 inversion recovery (STIR) sequence was performed with 6,885/72 (TR/TE) ms, 35 slices, a 4-mm section thickness, a field of view of 220×220 mm and a voxel size of $1.1 \times 0.7 \times 4.0$ mm. A transverse T1-weighted SE sequence was performed with 570/9.7 (TR/TE) 35 slices, 4-mm section thickness, a field of view of 220×220 mm and a voxel size of $1.1 \times 0.7 \times 4.0$ mm. Transverse echo-planar diffusion-weighted (DW) images were performed in the transverse plane before the contrast material injection with b values of 1,000 and 2,000. After that, coronal T1-weighted SE sequence was performed. Following the injection of gadolinium (Dotarem, Guerbet, France), T1-weighted sequence was repeated in axial, coronal and sagittal directions. Dedicated MR acquisition time was 27 min 8 s. Axial images of regional PET with MRI were parallel to anterior and posterior commissure line of the brain.

The maximum and average standardized uptake value (SUVmax and SUVmean) were used to determined FDG avidity of primary site and suspicious metastatic lymph nodes. Total lesion glycolysis was calculated by multiplying the SUVmean of the primary tumor by the volume of the primary tumor.

Interpretation of PET/MR

All PET and PET/MRI images were retrospectively interpreted jointly and in consensus by two experienced physicians trained in nuclear medicine. Patient information was

partially known to the interpreters. The images of whole-body PET only, whole-body PET/Dixon-VIBE MRI, regional PET only and regional PET/Gd-MRI were interpreted by two nuclear medicine physicians (S.J.L. and H.J.S.). The whole-body PET and regional PET images were analyzed from the monitor of the computer workstation on different days at 2-week intervals. Whole-body PET/Dixon-VIBE MRI images were analyzed after reading PET on whole-body PET reading day. Fusion image of PET/Dixon-VIBE and regional PET/Gd-MRI showed good alignment. Regional PET/Gd-MRI images were finally interpreted on regional PET reading day at the end. The interpreters were aware that the patients had been proven to have head and neck tumor or metastatic cervical lymph nodes. Initially, the attenuation-corrected PET images were reviewed in axial, coronal and sagittal planes with maximum intensity projection (MIP). Image quality of PET attenuated by MRI was good to evaluate lesion detection. Visual assessment was analyzed; for the detection of primary tumor, asymmetrical and discrete FDG uptakes in the oral cavity and pharynx were recorded and graded as benign or malignant. Symmetrical FDG uptake of anatomic structure such as vocal cord and muscle were thought as normal physiology, and excluded from the analysis. For the identification of lymph nodes, the presence of prominent FDG uptake in bilateral upper and lower neck area was considered a positive finding for metastatic lymph nodes, regardless of the lymph node size. In integration image of regional PET with Gd-MRI image, the determination of primary site and metastatic lymph node was combined for the visual assessment from PET image and Gd enhancement from MRI images regardless of the subcentimeter

size lymph nodes. In each PET image, maximum SUV and total lesion glycolysis of primary tumor and suspicious metastatic lymph nodes were analyzed. The retention index was calculated by subtracting the SUV at 1 h on whole-body PET from the SUV at 1.5 h on regional PET.

Contrast-enhanced CT (CE-CT) and dedicated MRI were analyzed from the monitor in the picture archiving and communication system (PACS). The analysis of CE-CT images was based on the reading reports. Dedicated MRI images were analyzed by a radiologist (J.H.K.). In MRI images, metastatic lymph nodes were classified as enhancement on T1-weighted image with Gd contrast [10, 11]. In CE-CT and dedicated MRI, metastatic lymph nodes were considered when a short-axis diameter is greater than 1 cm. In subcentimeter-sized lymph nodes, morphologic feature of malignancy of necrosis and indistinct margins indicating extranodal spread were classified as metastatic lymph nodes.

The criteria of tumor staging were based on the seventh edition of the AJCC classification system. The tumor stage was determined according to the size of the tumor, the depth of invasion, and the involvement of surrounding structures. The nodal stage was determined according to the size, number, and location of the lymph nodes. TN staging for CE-CT, dedicated-MRI and regional PET/Gd-MRI was analyzed. NM staging for whole-body PET and whole-body PET/Dixon-VIBE MR, and N staging for regional PET were analyzed.

Statistical Analysis

Data were analyzed with the use of a commercial statistics package (MedCalc 9.5, MedCalc Software, Mariakerke, Belgium, Version 12.0; SPSS, Chicago, IL). Summary data are presented as median and range. The nonparametric Wilcoxon signed ranks test was used to evaluate the differences of SUV_{max} values between on whole-body PET and regional PET. Significance was accepted for p values < 0.05.

Results

Discordant and Concordant Lesion Detection According to Whole-Body PET, Regional PET, Dedicated MRI and Regional PET/Gd-MRI

Whole-body PET and regional PET detected ten primary sites and compensated for a missed lesion on dedicated MRI. The total number of suspicious metastatic lymph nodes was 40. Whole-body PET and regional PET additionally detected 6 and 23 suspicious lymph node metastases, respectively. Regional PET only detected suspicious lymph nodes much more than whole-body PET and dedicated MRI (Fig. 1). Therefore,

two patients were upstaged by regional PET (patients 6 and 10). Sensitivities of identifying metastatic lymph nodes on lesion-based analysis are shown in Table 2.

TN staging was modified in three patients based on regional PET/Gd-MRI and M staging was decided by whole-body PET. From a single PET/MRI study, the treatment of choice was decided. Table 1 summarizes TNM staging of eight patients with malignant tumor. T staging was decided by dedicated MRI, but a case was corrected by regional PET (patient 4). N staging showed highly discordant results; dedicated MRI in one patient and by regional PET in two patients (patients 6 and 10). A case of unknown origin metastatic lymph node was diagnosed with left tonsillar cancer by whole-body PET and regional PET but not by dedicated MR image (Fig. 2, patient 4). There was no distant metastasis based on analysis of whole-body PET and whole-body PET/Dixon-VIBE MRI.

Two benign tumors were delineated as benign both in PET (whole-body and regional PET) and dedicated-MRI. Warthin tumor was well-defined margin and round shape in right parotid gland (Fig. 3, patient 2) on each image modality.

Image Quality and Parameters

Whole-body PET and regional PET attenuated by MRI showed good image quality to evaluate lesion detection. The alignments of fusion PET/Dixon-VIBE MRI and regional PET/Gd-MRI were matched correctly. The mean SUV_{max}, SUV_{mean} and total lesion glycolysis of primary tumor and metastatic lymph nodes were shown in Table 3. Lesions of primary tumor and suspicious metastasis were well detected on both the SUV_{max} value and visual analysis. Additionally, the retention index parameter could be measured. In primary tumor, 22 % retention index was measured by different time points of SUV_{max}. Also, lymph node metastases demonstrated 21 % retention index of SUV_{max}. The differences of SUV_{max} values between whole-body PET and regional PET are demonstrated in Fig. 4. Enhancement of Gd was useful to evaluate malignancy and lymph node metastases in dedicated MRI.

Discussion

In this study, we evaluated PET attenuated by MRI and the image quality of PET/MRI. Integrated PET/MRI showed good alignment and reliable lesion detection for head and neck cancer staging. Moreover, whole-body PET combined with regional PET/Gd-MRI was feasible and convenient for staging as a single study. Discordant results of lesion detection among whole-body PET, whole-body PET/Dixon-VIBE MRI, regional PET and dedicated MRI and regional PET/Gd-MRI might improve diagnosis. Also, both anatomic and

Fig. 1 Warthin tumor of right parotid gland in a 60-year-old man. **a** MIP image of whole-body ^{18}F -FDG PET. **b** Coronal HASTE T2-weighted image of the whole body. **c** Axial image of contrast-enhanced CT of the head. **d** Axial image of Gd-contrast enhanced T1-weighted image of the head. **e** Axial dedicated PET image of the head. **f** Axial VIBE image of the head. **g** Axial integrated PET image combined with axial VIBE image

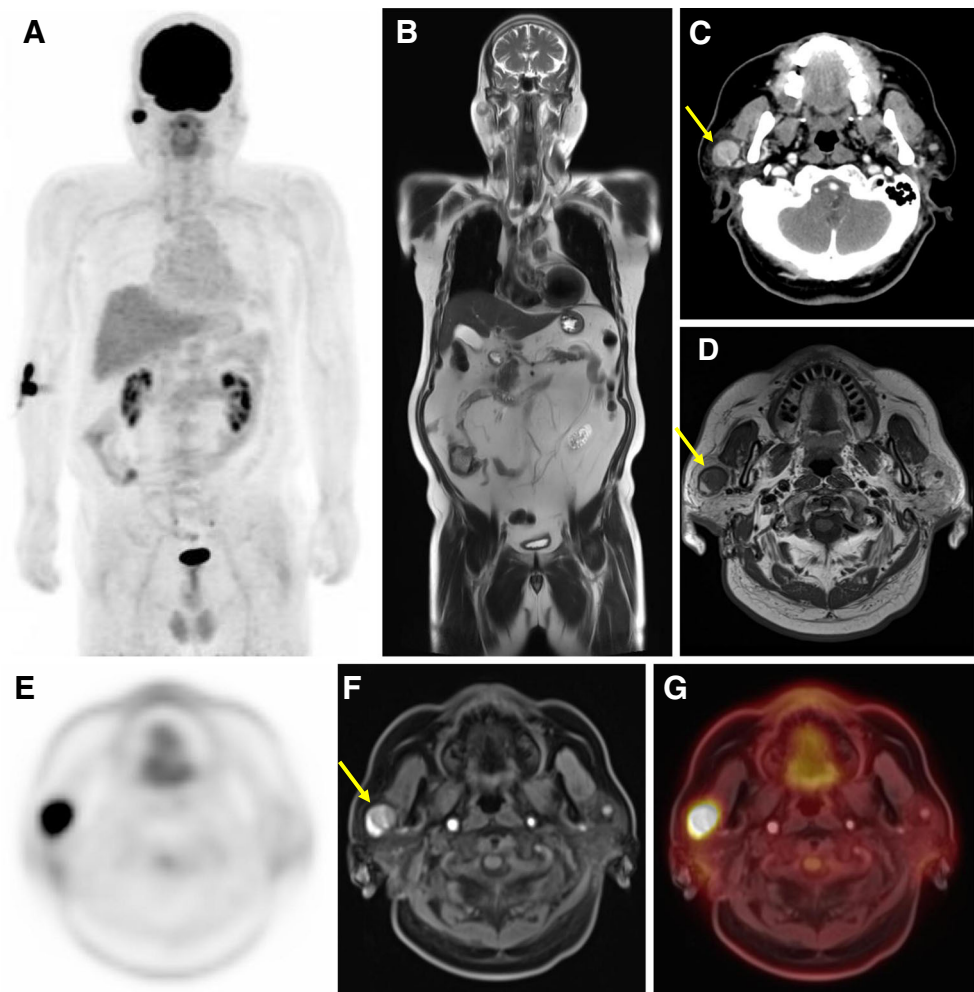


Table 2 Lesion-based sensitivity of whole-body PET, Gd-MRI, regional PET and regional PET/Gd-MRI

| | WB PET | Gd-MRI | R PET | R-PET/Gd-MRI |
|--|--------|--------|-------|--------------|
| Primary site in head and neck ^a | | | | |
| Primary site (<i>n</i> = 10) | | | | |
| Concordance | 10 | 9 | 10 | 10 |
| Discordance | 0 | 1 | 0 | 0 |
| Sensitivity | 100 % | 90 % | 100 % | 100 % |
| Suspicious lymph node metastases ^b | | | | |
| Suspicious lymph node metastases (<i>n</i> =40) | | | | |
| Concordance | 16 | 16 | 16 | 16 |
| Discordance | 6 | 0 | 23 | 24 |
| Sensitivity | 55 % | 40 % | 98 % | 100 % |

^a All primary lesions were confirmed by pathology (benign=2, malignant lesions=8)

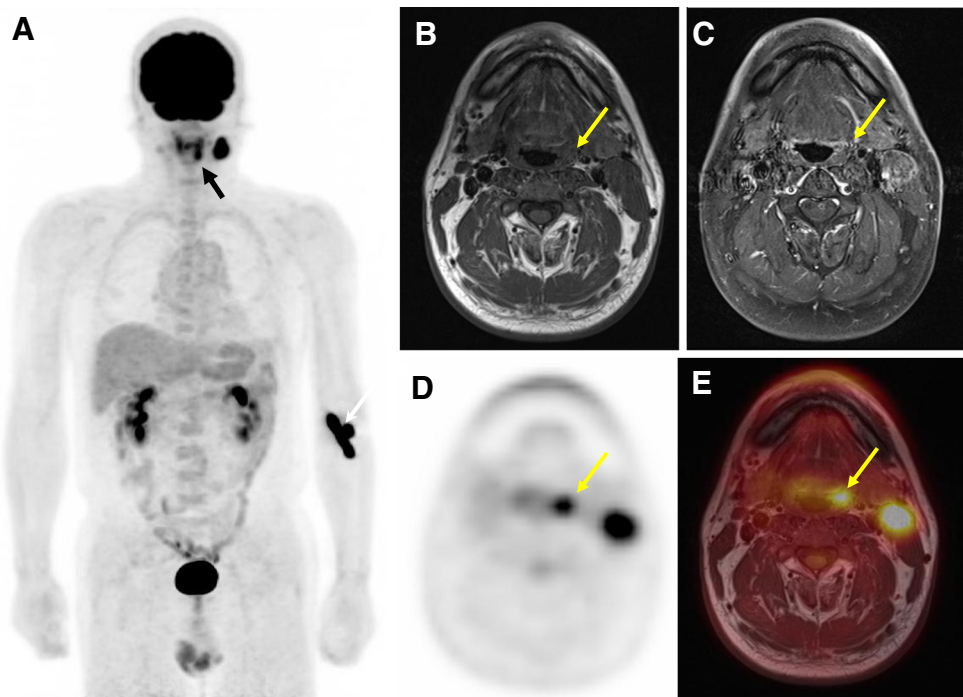
^b Total suspicious metastatic lymph nodes were 40. Five of 40 were confirmed by pathology (*n*=5) and the others (*n*=35) were confirmed by multimodal imaging and clinical decision. Coincidence or discordance was based on pathology, multimodal imaging and clinical decision. All pathological confirmed lesions (*n*=5) showed concordance

metabolic information using variable imaging parameters might show synergistic effects to localize and characterize lesions.

A total of ten primary sites and 40 suspicious metastatic lymph nodes were detected in ten patients. All ten primary lesions were detected on whole-body PET, regional PET and regional PET/Gd-MRI. The case of unknown origin tumor was corrected by PET as part of PET/MRI. Likewise, the sensitivity and specificity of PET has been known to be superior to CT and/or MRI in unknown primary tumors with cervical metastases [12]. Otherwise, as expected, MRI as part of PET/MRI had the great image quality to delineate the primary tumor relative to the surrounding soft tissue.

Subcentimeter lesions with avid FDG uptake were detected well in regional PET/Gd-MRI. Sixteen suspicious metastatic lymph nodes, including ones more than 1 cm and less than 1 cm, were all detected by the whole-body PET, dedicated MRI, regional PET and regional PET/Gd-MRI. An additional six and 24 suspicious lymph node metastases less than 1 cm were delineated only by whole-body PET and regional PET, respectively. Of subcentimeter lymph nodes in regional PET,

Fig. 2 Malignancy of unknown origin in a 54-year-old man (tonsillar cancer patient, patient 4 in Table 1). **a** MIP image of whole-body ^{18}F -FDG PET shows the asymmetrical metabolism in the pharynx (*black arrow*) and a biopsy proven metastatic lymph node in left neck. *White arrow* indicates the injection site of left arm. **b, c** Non-enhanced/contrast-enhanced T1-weighted axial images, respectively, did not show anatomical abnormality of the covered region. **d** Asymmetrically increased metabolism of the left tonsil. **e** Confirmation of the anatomical lesion primary site and metastatic lymph node. The left tonsillar tumor was confirmed by biopsy



significantly increased uptake was the critical finding to decide metastasis. However, all lesions were not confirmed by pathology and we did not have sufficient evidence of lymph node metastasis by follow-up image. Therefore, we mentioned suspicious lymph node metastases. But, the head and neck cancer patient with clinically N0 nodal staging has the possibility of false-negative in subcentimeter-sized lymph nodes [13, 14]. In this study, MRI as part of integrated PET/MRI improved anatomic localization of small lymph node metastases and avid FDG uptake enhanced diagnostic certainty as in

a previous report [15]. The integration of regional PET with MRI has potential to detect small lesions at an early stage.

Regional PET showed 18 more suspicious lymph nodes than whole-body PET. The additional effect of regional PET was based on a difference of acquisition time about triple that of whole-body PET and time delay between whole-body PET and regional PET. The acquisition of regional PET started with MRI per bed as soon as whole-body PET/Dixon-VIBE MRI was completed. The exam time of whole-body PET and regional PET was 3 and 10 min, respectively. And dual time

Fig. 3 Tonsillar cancer in a 72-year-old man (patient 6 in Table 1). **a** Coronal image of contrast-enhanced T1-weighted image. MIP images of whole-body (**b**) and regional ^{18}F -FDG PET (**c**). Coronal images of whole-body (**d**) and regional ^{18}F -FDG PET (**e**)

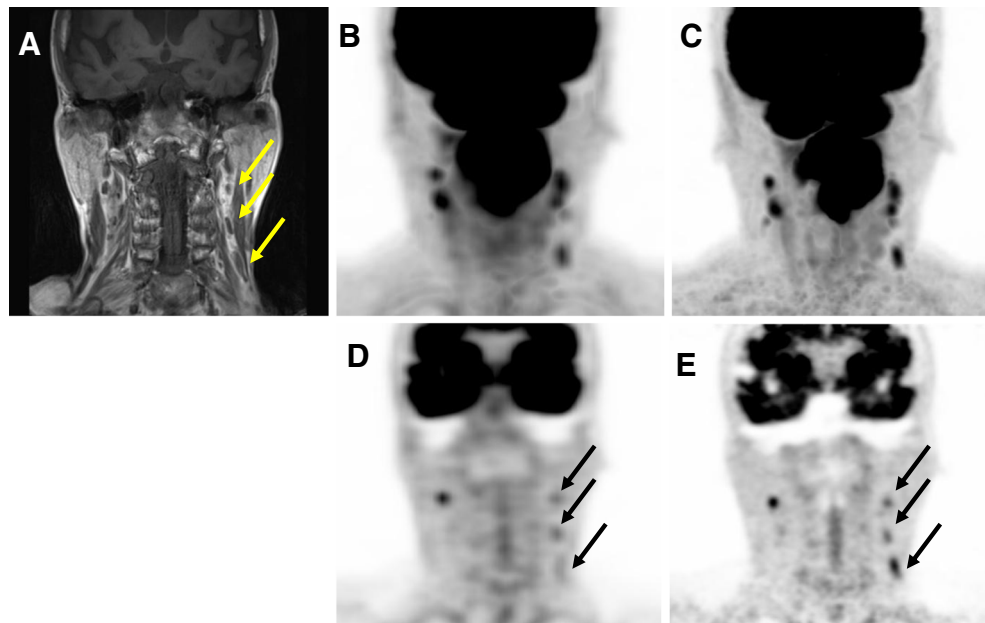


Table 3 SUV and total lesion glycolysis values in the primary tumors and metastatic lymph nodes

| | Whole-body PET | | Regional PET | |
|--|----------------|-----------|---------------------|-----------|
| | Median | Range | Median ^c | Range |
| Primary tumor, SUV | | | | |
| SUVmax | 11.1 | 6.3–20.8 | 13.5 (122 %) | 7.9–24.8 |
| SUVmean | 6.6 | 3.7–11.9 | 8.0 (121 %) | 4.6–13.8 |
| Nodal metastasis, SUV ^a | | | | |
| SUVmax | 7.6 | 2.3–14.0 | 9.3 (122 %) | 3.3–15.0 |
| SUVmean | 5.3 | 1.8–9.4 | 6.1 (115 %) | 2.1–10.3 |
| Total lesion glycolysis ^b (primary tumor) | 51.1 | 9.7–765.2 | 91.5 (179 %) | 9.1–667.9 |

^a One of them with SUVmax value among suspicious metastatic lymph nodes from each patient

^b Calculated tumor volume with 40 % threshold of SUVmax value

^c Increase from whole-body PET *in parentheses* refers to numerical value

points of whole-body PET at 1 h and regional PET at 1.5 h was useful to evaluate lymph node metastasis showing better tumor to normal count density ratio similar to previous reports [16, 17].

Combined information from multiple modalities increases diagnostic accuracy. Several studies have reported that combined-modality PET/CT is superior to dedicated PET or CT alone in head and neck cancer staging [2]. PET/CT reduces the number of indeterminate lymph nodes using better anatomic correlation compared with PET. MRI has the advantage

in soft-tissue characterization even without application of contrast agent and reduces the radiation exposure, which is another good modality replacing CT as part of PET/CT. Moreover, regional PET increases detection of metastatic lymph node and changes staging. PET/MRI is good for the staging in head and neck cancer and is convenient for a single modality. Also, the advantage of whole-body PET/MRI image can be applied for systemic evaluation as a single method. Whole-body PET/MRI has the advantage to detect both TNM staging and distant metastasis at the same time. MRI scanner is a device using nuclear magnetic resonance to image nuclei of atoms. It produces the differential images from several sequences, which were useful to evaluate lesions in this study [18]. In this study, no patient has evidence of distant metastasis from whole-body PET and whole-body PET/Dixon-VIBE MRI images. However, more studies for this synergistic effect of PET and MRI sequences should be studied.

Our study has some limitations. We discussed ten preliminary cases of patients with head and neck cancer. Further studies are expecting to discuss the detailed analysis in large population. Second, all suspicious metastatic lymph nodes were not proven by histopathology. After PET/MRI scan, seven patients were treated with chemotherapy and radiotherapy. There was no sufficient time to observe those clinical processes. Third, the motion artifact to be influenced by respiration was not mentioned on MRI. The image of organs such as lung, diaphragm and liver could be distorted by MRI. The artifacts of dental implants in the oral cavity were induced. These artifacts have less an effect on reading PET, while greatly influencing MRI [19]. Fourth, the most negative

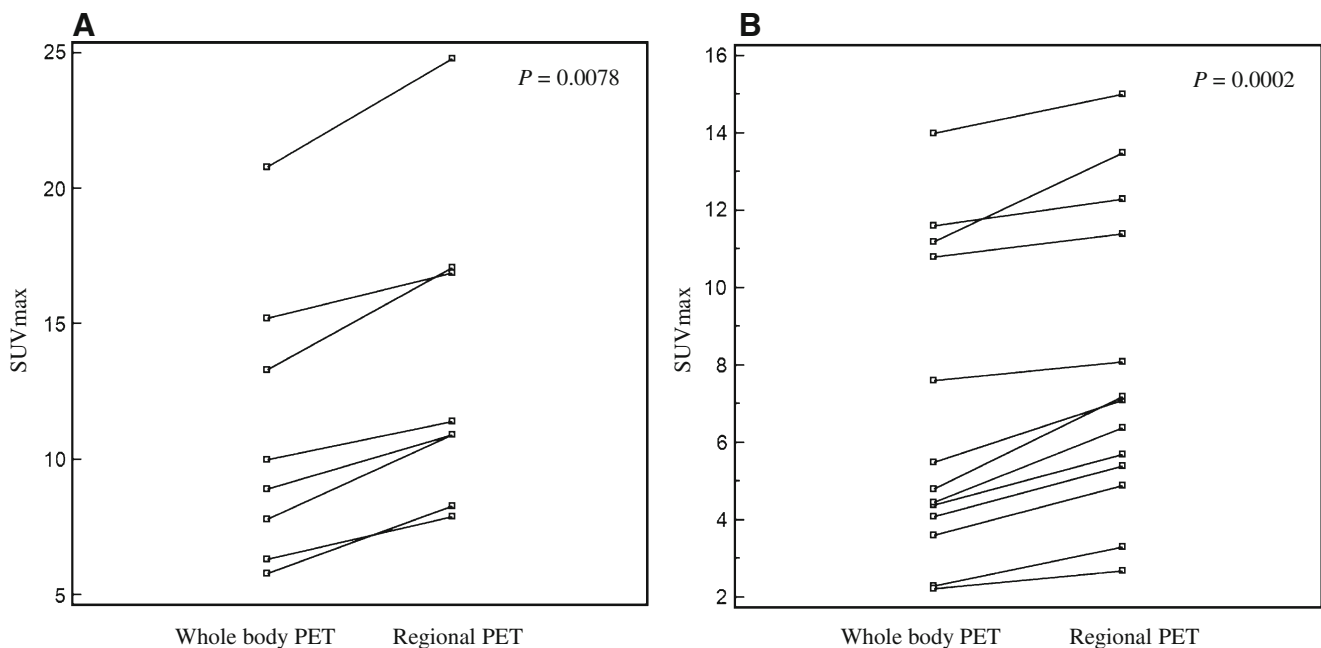


Fig. 4 The differences of SUVmax values between on whole-body PET and regional PET. Primary tumors (a) and multiple suspicious lymph node metastases (b) show a tendency of further increased FDG uptake in regional PET

element of PET/MRI was the prolonged examination time. It took about 1 h to obtain whole-body PET/Dixon-VIBE MRI and Gd-MRI, except for the preparation time between MRI sequences. Half the time was due to various MRI sequential images. It needs to reduce the examination time in purpose of facilities of use. The best sequence of MRI should be considered for clinical use, except unnecessary sequences. Five, variable imaging parameter such as SUVmax, SUVmean, TLG, retention index and ADC can be measured in routine integrated PET/MRI. Further specific study of these parameters should be interpreted.

Conflict of interest Soo Jin Lee, Hyo Jung Seo, Gi Jeong Cheon, Ji Hoon Kim, E. Edmund Kim, Keon Wook Kang, Jin Chul Paeng, June-Key Chung, Dong Soo Lee declare that they have no conflict of interest.

References

- Pauleit D, Zimmermann A, Stoffels G, Bauer D, Risse J, Fluss MO, et al. 18F-FET PET compared with 18F-FDG PET and CT in patients with head and neck cancer. *J Nucl Med*. 2006;47:256–61.
- Branstetter BF, Blodgett TM, Zimmer LA, Snyderman CH, Johnson JT, Raman S, et al. Head and neck malignancy: is PET/CT more accurate than PET or CT alone? *Radiology*. 2005;235:580–6.
- In: National Comprehensive Cancer Network. <http://www.nccn.org>.
- Yoon DY, Hwang HS, Chang SK, Rho YS, Ahn HY, Kim JH, et al. CT, MR, US, F-18-FDG PET/CT, and their combined use for the assessment of cervical lymph node metastases in squamous cell carcinoma of the head and neck. *Eur Radiol*. 2009;19:634–42.
- Goerres GW, von Schulthess GK, Hany TF. Positron emission tomography and PET CT of the head and neck: FDG uptake in normal anatomy, in benign lesions, and in changes resulting from treatment. *AJR Am J Roentgenol*. 2002;179:1337–43.
- Ratib O, Beyer T. Whole-body hybrid PET/MRI: ready for clinical use? *Eur J Nucl Med Mol I*. 2011;38:992–5.
- Platzek I, Beuthien-Baumann B, Schneider M, Gudziol V, Langner J, Schramm G, et al. PET/MRI in head and neck cancer: initial experience. *Eur J Nucl Med Mol I*. 2013;40:6–11.
- Pfluger T, Melzer HI, Mueller WP, Copenrath E, Bartenstein P, Albert MH, et al. Diagnostic value of combined F-18-FDG PET/MRI for staging and restaging in paediatric oncology. *Eur J Nucl Med Mol I*. 2012;39:1745–55.
- Quick HH, von Gall C, Zeilinger M, Wiesmuller M, Braun H, Ziegler S, et al. Integrated whole-body PET/MR hybrid imaging clinical experience. *Invest Radiol*. 2013;48:280–9.
- Sumi M, Sakihama N, Sumi T, Morikawa M, Uetani M, Kabasawa H, et al. Discrimination of metastatic cervical lymph nodes with diffusion-weighted MR imaging in patients with head and neck cancer. *AJNR Am J Neuroradiol*. 2003;24:1627–34.
- de Bondt RB, Nelemans PJ, Bakers F, Casselman JW, Peutz-Kootstra C, Kremer B, et al. Morphological MRI criteria improve the detection of lymph node metastases in head and neck squamous cell carcinoma: multivariate logistic regression analysis of MRI features of cervical lymph nodes. *Eur Radiol*. 2009;19:626–33.
- Regelink G, Brouwer J, de Bree R, Pruim J, van der Laan BFAM, Vaalburg W, et al. Detection of unknown primary tumours and distant metastases in patients with cervical metastases: value of FDG-PET versus conventional modalities. *Eur J Nucl Med Mol I*. 2002;29:1024–30.
- Byers RM, El-Naggar AK, Lee YY, Rao B, Fornage B, Terry NHA, et al. Can we detect or predict the presence of occult nodal metastases in patients with squamous carcinoma of the oral tongue? *Head Neck J Sci Spec*. 1998;20:138–44.
- Schoder H, Carlson DL, Kraus DH, Stambuk HE, Gonen M, Erdi YE, et al. F-18-FDG PET/CT for detecting nodal metastases in patients with oral cancer staged N0 by clinical examination and CT/MRI. *J Nucl Med*. 2006;47:755–62.
- Nagarajah J, Jentzen W, Hartung V, Rosenbaum-Krumme S, Mikat C, Heusner TA, et al. Diagnosis and dosimetry in differentiated thyroid carcinoma using I-124 PET: comparison of PET/MRI vs PET/CT of the neck. *Eur J Nucl Med Mol I*. 2011;38:1862–8.
- Abgral R, Le Roux PY, Rousset J, Querellou S, Valette G, Nowak E, et al. Prognostic value of dual-time-point 18F-FDG PET-CT imaging in patients with head and neck squamous cell carcinoma. *Nucl Med Commun*. 2013;34:551–6.
- Kubota K, Yokoyama J, Yamaguchi K, Ono S, Qureshy A, Itoh M, et al. FDG-PET delayed imaging for the detection of head and neck cancer recurrence after radio-chemotherapy: comparison with MRI/CT. *Eur J Nucl Med Mol Imaging*. 2004;31:590–5.
- Castelijns JA. PET-MRI in the head and neck area: challenges and new directions. *Eur Radiol*. 2011;21:2425–6.
- Baek CH, Chung MK, Son YL, Choi JY, Kim HJ, Yim YJ, et al. Tumor volume assessment by F-18-FDG PET/CT in patients with oral cavity cancer with dental artifacts on CT or MR images. *J Nucl Med*. 2008;49:1422–8.